Luminescence properties of $Cu_2ZnSn(S,Se)_4$ solar cell absorbers: State filling versus screening of electrostatic potential fluctuations

Mario Lang,[1] Christian Zimmermann,[1,*] Christoph Krämmer,[1] Tobias Renz,[1] Christian Huber,[1] Heinz Kalt,[1] and Michael Hetterich[1,2]

[1]*Institute of Applied Physics, Karlsruhe Institute of Technology (KIT), 76131 Karlsruhe, Germany*

[2]*Light Technology Institute, KIT, 76131 Karlsruhe, Germany*

(Received 23 December 2016; published 13 April 2017)

The power conversion efficiency of $Cu_2ZnSn(S,Se)_4$ kesterite thin-film solar cells is mainly limited by a low open-circuit voltage V_{OC}. In the literature, this low V_{OC} has been amongst others attributed to electrostatic potential fluctuations leading to fluctuating band edges. This assignment was mainly based on the observation of a shift of the photoluminescence (PL) maximum to higher photon energies as a function of excitation power, which was interpreted in terms of a screening of the electrostatic potential fluctuations. However, in this paper, we show evidence that the observed shift of the PL maximum is dominantly caused by state filling rather than screening. Our assignment is based on the investigation of the full PL line shape (not only of the PL maximum) and the PL yield as a function of excitation power and temperature. Further support of our interpretation is given by the observation of additional band-tail emission showing up as a second high-energy PL band at the highest excitation powers. The spectral position of this additional band coincides with the absorption-tail deduced from photoluminescence excitation spectroscopy (PLE).

DOI: 10.1103/PhysRevB.95.155202

I. INTRODUCTION

In comparison to the established absorber materials $Cu(In,Ga)(S,Se)_2$ and CdTe for thin-film solar cells, devices based on kesterite absorbers such as $Cu_2ZnSn(S,Se)_4$ (CZTSSe) require less toxic and scarce constituents. While for the two technologies mentioned first, power conversion efficiencies approaching 23% [1,2] ($Cu(In,Ga)Se_2$) and 22.1% [3] (CdTe) have been achieved, the maximum power conversion efficiency realized for CZTSSe thin-film solar cells is only 12.6% [4]. The latter is mainly limited by the low open-circuit voltage (V_{OC}) of the devices compared to the value expected with respect to the band gap of the absorber material.

The open-circuit voltage V_{OC} is particularly affected by recombination within the thin-film solar cell device [5]. In the detailed balance considerations of Shockley and Queisser, only radiative recombination is taken into account [6]. However, other recombination paths like nonradiative recombinations are also present and reduce the V_{OC} and hence the efficiency. Due to these additional recombination paths, the quasi-Fermi level splitting is reduced and the V_{OC} is lowered. The V_{OC} is also reduced if inside the absorber material the band gap is not constant. One reason for this could be the incorporation of secondary phases [7]. Further reasons could be an inhomogeneous distribution of S/Se, nonuniform strain [8] or disorder, e.g., within the Cu–Zn planes as reported by several authors [9–14]. Due to Scragg *et al.*, Cu–Zn disorder leads to large fluctuations of the individual band edges and the corresponding band gap and could be the cause for a large V_{OC} deficit and a reduced power conversion efficiency [7,15]. In contrast to fluctuations of the local band gap, electrostatic potential fluctuations (EPFs) do not alter the local band gap. Rather, the valence and the conduction band edges fluctuate in parallel to each other. These EPFs could also reduce the open-circuit voltage [5,8]. Since CZTSSe absorber layers used in thin-film solar cells are highly off-stoichiometric (Cu-poor and Zn-rich) [4,5], one can expect a high density of charged defects and a high degree of compensation and therefore the existence of EPFs [16,17].

As stated above, there are several mechanisms that can reduce the V_{OC}, but it is not clear which is the dominant one in CZTSSe. Especially, the influence of band gap fluctuations and of EPFs is largely discussed, not only on the open circuit voltage but also on the properties of CZTSSe in general [8,15,18]. There are several studies on CZTSSe absorber layers using simulations [19] or optical and electrical characterization techniques, e.g., photoluminescence (PL) spectroscopy [17,20–23], time-resolved PL spectroscopy [8], and current-voltage measurements [24], which attribute their findings to the existence of band gap fluctuations and/or EPFs. However, the distinction between these two kinds of band edge fluctuations is not straightforward. PL studies in dependence of excitation power and temperature are often used to attribute the band edges fluctuations to EPFs [20,21]. This attribution is usually made based on the shifting behavior of the PL maximum with increasing excitation power [20,21]. For an increase in excitation power at a constant temperature, a large shift of the PL maximum towards higher photon energies is observed. Assuming the existence of EPFs the large shift can be explained by screening of these local potential fluctuations [25].

We propose in this paper that screening is not suitable to explain the properties of the PL. In order to prove our proposal, we investigated the radiative recombination at low temperatures in CZTSSe absorber layers of finished thin-film solar cells. We compare the results to expectations from different luminescence models. Furthermore, we use photoluminescence excitation (PLE) spectroscopy to obtain more information about the nature of the radiative transitions and about the tailing character of the band edge. From these

*Current address: Department of Physics/Center for Materials Science and Nanotechnology, University of Oslo, P.O. Box 1048 Blindern, N-0316 Oslo, Norway.

considerations we conclude that state filling is the suitable effect to explain the properties of the PL.

II. EXPERIMENTAL METHODS

Polycrystalline CZTSSe thin-film solar cell devices with the standard layer sequence ZnO:Al/i-ZnO/CdS/CZTSSe on Mo-coated soda-lime glass were fabricated as described by Schnabel *et al.* [26] utilizing a wet-chemical approach and a subsequent annealing in a Se atmosphere. The corresponding CZTSSe absorber layers are Cu-poor and Zn-rich with a ([S]/([S]+[Se])) ratio of approximately 10%.

The investigated CZTSSe thin-film solar cells were post-annealed in a rapid-thermal processing system to increase the degree of order within the Cu–Zn planes of the corresponding CZTSSe absorber layer [12,14]. For this purpose, the sample representatively discussed in the following was heated up to 150 °C for 2 h and afterwards cooled-down slowly to room temperature with a rate of 2 K/h as described by Krämmer *et al.* [27]. The higher degree of order within the Cu–Zn planes leads to a larger band gap of the CZTSSe absorber layer [13,14,27]. This is accompanied by a shift of the radiative recombination measured at low temperatures towards higher photon energies [28,29]. In principle the recombination channel can also change with varying degree of Cu–Zn order, but since the PL maximum shifts in parallel to the band gap the shift of the main radiative transition is mainly determined by the change in band gap energy [29]. The band gap of the presented CZTSSe solar cell absorber layer is 1.07 eV at room temperature as determined by electroreflectance spectroscopy (ER). Details on this technique and its application to thin-film solar cells can be found in Refs. [30,31].

A wavelength-filtered laser diode ($\lambda = 670$ nm) was used for PL excitation. The excitation was intensity-modulated using a chopper wheel with a frequency of approximately 210 Hz in order to utilize a lock-in amplifier for low-noise detection of the PL signal. The spectrum was dispersed by a 0.64-m focal length monochromator ($NA \approx 0.1$) and detected by a liquid-nitrogen cooled electronically amplified InGaAs photodiode. The monochromator was purged with N_2 during measurements to lessen distortions caused by water vapor absorption in the IR spectral region. During the PL measurements the samples were mounted in a He bath cryostat to allow for temperature-dependent measurements. PL spectra were corrected with respect to the spectral response of the detector and fitted using an empirical asymmetric double sigmoidal function as proposed by Krustok *et al.* [32]:

$$I(\hbar\omega) \propto \left[\frac{1}{1+\exp\left(-\frac{\hbar\omega-E_1}{W_1}\right)}\right]\left[1-\frac{1}{1+\exp\left(-\frac{\hbar\omega-E_2}{W_2}\right)}\right]. \tag{1}$$

$E_{1,2}$ and $W_{1,2}$ are experimental fitting parameters with no direct physical meaning [32]. The sole purpose of this fitting procedure is to accurately extract the PL maximum $E_{\max}$ and the integrated PL yield Y [32,33]. It should be emphasized that at this point no assumption on the underlying physical recombination processes is made yet.

For PLE measurements, the excitation photon energy is varied while the detection photon energy is held constant [34]. PLE has the advantage that it can—in comparison to, e.g., transmission measurements—be performed on finished solar cell devices. A 250-W quartz-tungsten halogen lamp in combination with a 0.32-m focal length monochromator ($NA \approx 0.12$) served as a light source with a tunable emission photon energy. The detection was performed using the same monochromator and detector as in the case of the PL measurements. Since the excitation intensity could not be held completely constant during a PLE measurement (intensity dependence of the halogen lamp) the line shape of the PL spectra detected at different excitation energies (with the same light source as used for the PLE measurements) was investigated beforehand. A constant line shape is important to exclude nonlinear effects between the PLE intensity and the excitation intensity and a nearly constant relaxation probability [35]. Afterwards, PLE spectra were corrected for the photon energy-dependent excitation intensity of the light source, the detector response and the PL intensity at different detection wavelengths λ_{det}. PLE measurements were solely performed at a temperature of $T = 10$ K, due to the low excitation power and the low luminescence yield at higher temperatures.

III. RESULTS

Our aim with this manuscript is to distinguish between screening of EPFs and state filling as the dominant mechanism for the radiative recombination behavior. Additionally, we want to get more information about the nature of the radiative transition and the tailing character of the absorption. Therefore power- and temperature-dependent PL measurements (and a combination of both) as well as PLE measurements were performed. A detailed discussion of the results and the theoretical background needed to classify them is thoroughly presented in Sec. IV.

A. Power-dependent photoluminescence

Figure 1 shows logarithmically plotted PL spectra, which were measured at different excitation powers P.

With increasing P a shift of the high-energy tail towards higher photon energies is observed. This shift of the high-energy tail is accompanied by a shift of the PL maximum to higher photon energies, while both the low-energy and the high-energy tail do not change their slope.

Several authors use the following relation to describe the shift of the PL maximum $E_{\max}$ with increasing P [20,21,36–38]:

$$P \propto \exp\left(\frac{E_{\max}}{\beta}\right), \tag{2}$$

where β represents the energetic shift of $E_{\max}$ in a certain range of varied excitation power. In Fig. 2(a), $E_{\max}$ is plotted over $\log_{10}(P)$ to determine the energetic shift β_{dec} of $E_{\max}$ per decade of varied P [β_{dec} is related to β of Eq. (2) via $\beta_{\text{dec}} = \frac{\beta}{\log_{10}(e)}$]. A value of $\beta_{\text{dec}} = 14.5 \pm 0.5$ meV/decade was determined. The indicated error is the standard deviation of the linear fit to the data points. The value for β_{dec} is in accordance with values already published by other groups [20,21,37,38].

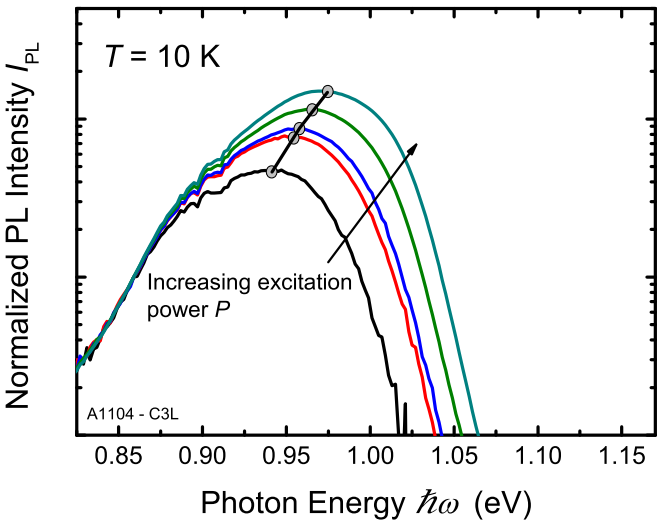

FIG. 1. Logarithmically plotted PL spectra for different nominal excitation powers P. All spectra were normalized to a value on their corresponding low-energy side ($\hbar\omega \approx 0.86$ eV). With increasing P, a shift of the high-energy tail towards higher photon energies can be observed. The slope of the low-energy side does not change with increasing P. The gray dots indicate the maximum of the PL determined from the fit of Eq. (1) to the PL spectra.

To get a hint about the physical nature of the observed radiative transition the so-called k value can be used. k is obtained using the following relation between the integrated PL yield Y and P [39]:

$$Y \propto P^k. \tag{3}$$

The value for k depends not only on the observed nature of the radiative transition but also on the temperature, the doping of the material and the excitation regime [40,41]. A value of $k < 1$ is observed and calculated in free-to-bound

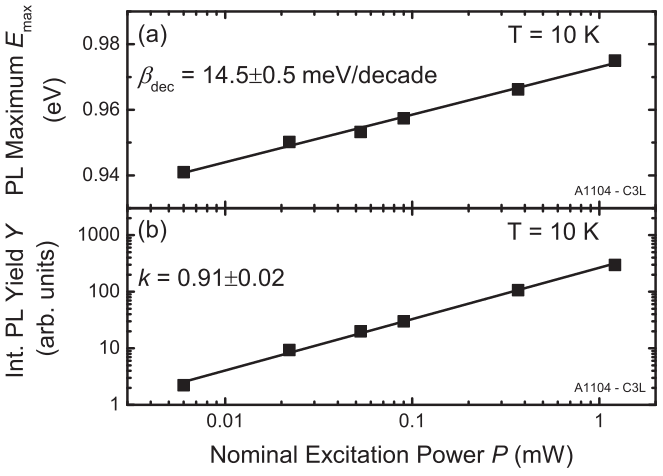

FIG. 2. (a) PL maximum E_{max} in dependence of $\log_{10}(P)$. A linear fit to the data points yields the energetic shift β_{dec} of the PL maximum E_{max} per varied decade of nominal excitation power P. A value of $\beta_{dec} = 14.5 \pm 0.5$ meV/decade was obtained. (b) A linear fit to a double-logarithmic plot of the power-dependent PL yield Y results in a k value of $k = 0.91 \pm 0.02$.

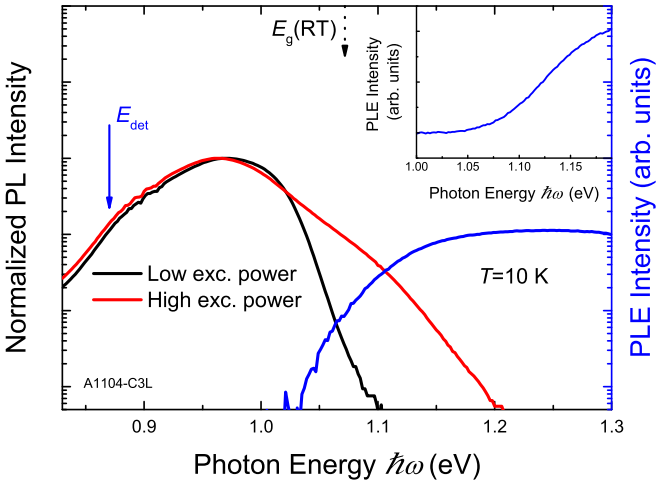

FIG. 3. Comparison of logarithmically plotted PL spectra and a logarithmically plotted PLE spectrum. The inset shows the tail region of the PLE spectrum on a nonlogarithmic scale. The PL spectrum recorded at a higher nominal excitation power P (red) shows two contributions. While the low-energy contribution lies energetically far below the PLE spectrum (blue), the high-energy contribution is situated within the tail of the PLE spectrum. The low-energy contribution is also visible in the case of a lower P (black). The dotted arrow indicates the energetic position of the band gap measured with electroreflectance at room temperature.

and in donor-acceptor pair transitions. Hence transitions with $k < 1$ normally involve states which are not related to the unperturbed conduction and valence band [39]. Figure 2(b) shows a double-logarithmic plot of the dependence of the PL yield Y on P. The slope of a linear fit yields $k = 0.91 \pm 0.02$ (error is the standard deviation of the linear fit), which suggests, that the observed radiative transition is indeed not directly related to the unperturbed valence and conduction band [39]. However, as already stated above, this value alone is not sufficient to get a clear assignment of the PL emission to the physical nature [40,41]. Furthermore, Schmidt *et al.* did not explicitly calculate the influence of band gap and/or electrostatic potential fluctuations on the PL power dependence [39]. Nevertheless, the determined k value indicates a transition which is rather related to traplike states induced by material imperfections.

B. Photoluminescence excitation

To further clarify the origin of the radiative transition, a comparison of the complementary techniques PL and PLE is useful. Figure 3 shows a logarithmically plotted PLE spectrum detected at a photon energy of $\hbar\omega = 0.87$ eV in comparison to logarithmically plotted PL spectra recorded with different excitation powers P. The PLE spectrum shows a tail to low photon energies (see inset of Fig. 3). The shape of the tail cannot be described by a single exponential behavior as proposed by Urbach [42], but can be modeled by more complicated relations. For instance, a model proposed by Katahara and Hillhouse or a model proposed by Gokmen *et al.* based on a Gaussian distribution of the local band gap as

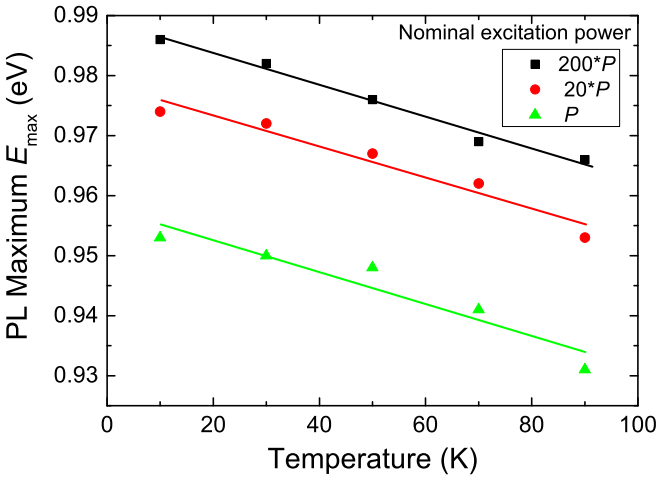

FIG. 4. PL maximum as a function of temperature for different excitation powers. A linear shift of the PL maximum to lower energies is observed with increasing temperature. The slope of the shift is independent of the excitation power which was varied over more than two orders of magnitude.

defined by Mattheis *et al.* can be used to model the shape of the tail [8,43,44].

In principle, PLE spectra display the absorption of a material but this can be distorted by energy dependent nonradiative recombination. To exclude energy dependent nonradiative recombination PL spectra taken with different excitation energies were compared. Furthermore, PLE spectra taken at different detection energies were also compared. Since the PL spectra as well as the PLE spectra show comparable line shapes, respectively, the difference in nonradiative recombination in the energetic region of the tail states should be negligible and together with the afore-mentioned corrections applied to the measured PLE spectra the corrected PLE spectra are considered to be essentially proportional to the absorption coefficient [34,45].

For high values of P, a second contribution is visible at the high-energy side of the PL spectra. This contribution lies energetically within the tail of the PLE spectrum. Actually, it also lies in the region where the band gap has been determined by the independent technique of electroreflectance.[1] The low-energy contribution, which can be seen in both PL spectra is situated energetically far below the PLE spectrum.

C. Temperature-dependent photoluminescence

Figure 4 shows the behavior of the PL maximum with varying temperature for three different excitation powers. The plotted lines are linear fits to the data points. The corresponding slope does not change significantly as a function of the excitation intensity, which is varied over more than two orders of magnitude. This means that the shift to higher energies with increasing P does not depend on temperature. Higher temperatures than $T = 90$ K are not considered since for such temperatures the high-energy side clearly shows a second contribution, which makes it impossible to further investigate the shifting behavior of the low-energy contribution.

IV. LUMINESCENCE THEORY OF KESTERITES AND DISCUSSION OF RESULTS

In the following the results of Sec. III are analyzed and discussed in the context of already published work. We show evidence that the observed luminescence behavior is due to a state filling and not due to a screening effect.

The following section is splitted into several parts. First, we analyze the PL data with respect to the absorption deduced from PLE. This is done to get more information about the luminescence origin and about the density of states responsible for luminescence. In the second paragraph, we try to classify the luminescence of $Cu_2ZnSn(S,Se)_4$ into the existing models. Before we compare our experimental results with the theoretical expectations of a state filling and a screening effect in the last paragraph we determine how state filling can in principle be distinguished from a screening effect with the used measurement techniques.

A. Luminescence compared to absorption in CZTSSe

In the first paragraph, the luminescence signal will be analyzed with respect to the PLE which describes the absorption of the investigated solar cell. The main PL recombination path at $T = 10$ K can be identified as a transition which is energetically situated far below the absorption edge as measured with PLE which means that there is only little absorption in the energetic region where the luminescence is created. Therefore the luminescence is not related to a conduction band to valence band transition (also indicated by a k value of $k < 1$), as expected in a perfect and defect free semiconductor.

1. Luminescence origin of CZTSSe

Since the composition of the CZTSSe is typically off-stoichiometric and intrinsically $Cu_2ZnSn(S,Se)_4$ absorber layers show the so-called Cu–Zn disorder the defect density is expected to be very high [15,19]. Despite the post-annealing procedure, the amount of defects related to Cu–Zn disorder is still high and in the order of $N \approx 10^{20}$–10^{21} cm^{-3} [15,46]. Also the amount of other defects like V_{Cu} is expected to be high. Due to the high amount of defects, it is generally not valid to talk about separate and isolated defects anymore [47]. The defects rather form bands or can even be considered as being part of the crystal structure as already considered by other groups [15]. For a high defect density, the defect levels can also merge with the initial bands [48]. Unfortunately, we do not know the exact distribution of the density of the different defects and their specific influence on the microstructure. However, their influence on macroscopic parameters like the band gap and the band tailing can be investigated [46].

If the excitation power is raised, a shoulder in the PL appears, which coincides energetically with the absorption-tail deduced from PLE measurements. Hence the PL at high

[1]It has to be mentioned that the band gap changes only little as a function of temperature. Only a small increase of the band gap of CZTSe of around $\Delta E_g \approx 20$ meV was found decreasing temperature from $T = 350$ to 50 K [59].

excitation power is band-tail-related. To be more precise, we define the band tail in this manuscript as the tail we see in PLE and hence in absorption. Since we see it in absorption, the joint density of states (JDOS) within this tail is rather high and therefore, it is formed due to a tailing of the valence and/or conduction bands. This is also consistent with the fact that the band gap measured with electroreflectance lies energetically in the tail region, suggesting a large JDOS.

Due to the fact that the absorption derived from PLE is very low in the energetic region of the PL at low excitation power, the joint density of states in this region is also rather low. Hence this JDOS differs from the one described above and the two densities have different nature. In contrast to the JDOS described above, which is related to the bands, the low-energy JDOS is related to traplike states induced by material imperfections. This is consistent with the fact that the PL is situated energetically far below the absorption edge and with a k value $k < 1$.

2. Modeling the absorption in CZTSSe

A closer look at the PLE spectrum reveals that the band tail cannot be described by a single exponential as proposed by the so-called Urbach model [42]. However, other more extensive models can be used to describe the tailing. As already mentioned, fluctuations of the local band gap are likely in kesterite materials due to, e.g., clustering of $[Cu_{Zn} + Zn_{Cu}]$ antisites induced by disorder [15]. Assuming a Gaussian distribution for the local band gap the absorption coefficient in a direct band gap semiconductor with parabolic bands can be expressed as [8,44]

$$\alpha(\omega) \propto \frac{1}{\gamma\hbar\omega}\int_0^\infty \exp\left[-\frac{1}{2}\left(\frac{E-\bar{E}_g}{\gamma}\right)^2\right]\sqrt{\hbar\omega - E}\,dE, \tag{4}$$

with γ being the standard deviation of the band gap distribution with the mean band gap value $\bar{E}_g$. This variation in the band gap results in a tailing of the absorption coefficient. A tailing depth of $\gamma \approx 34$ meV was determined. Other inhomogeneities such as randomly distributed charged defects can also result in an exponential distribution of band-tail states and hence a tail in the absorption coefficient [49]. The exact exponential dependence differs for the various used models. Fitting the PLE data with the different models alone is not sufficient to differentiate between the mechanisms (e.g., band gap fluctuations from EPFs) since the PLE data lacks characteristic features. However, our aim is not to clearly determine the origin of the tailing since both kinds of fluctuations can be expected to be present simultaneously in CZTSSe to some extent. Instead, we want to determine the main physical reason for the observed behavior of the PL as a function of excitation power.

We have seen in the above discussion that luminescence at low temperature and not too high excitation power is due to a transition, which is situated energetically below the absorption edge. At high excitation power, a second contribution to the PL is observed which is related to the band tail. The origin of the tail cannot be determined unambiguously but models accounting for band gap fluctuations or EPFs can be used to describe the tailing which shows a tailing parameter $\gamma \approx 34$ meV.

B. Luminescence models

Since the low excitation power luminescence is related to traplike states induced by material imperfections, we will in the following compare the PL with different existing luminescence models to get some more detailed understanding of the luminescence origin.

1. Donor-acceptor pair transitions

Excitation power-dependent PL measurements show a β_{dec} value of $\beta_{dec} = 14.5 \pm 0.5$ meV/decade. For pure donor-acceptor pair transitions (DAP transitions) such a large value of β_{dec} cannot be explained. The maximum shift of the PL maximum $\Delta E_{max,shift}$ to higher energies in DAP transitions can be estimated by [50,51]

$$\Delta E_{max,shift} = \frac{e^4 m_e^*}{(2[4\pi\epsilon_0\epsilon_r\hbar]^2)}, \tag{5}$$

with the effective electron mass m_e^*. The other symbols have their usual meanings. The maximum shift for Cu_2ZnSnS_4 with $m_e^*(S) \approx 0.18\,m_0$ and $\epsilon_r(S) \approx 6.8$, and $Cu_2ZnSnSe_4$ with $m_e^*(Se) \approx 0.08\,m_0$ and $\epsilon_r(Se) \approx 8.6$ [54] is calculated with the above relation to $\Delta E_{max,shift} \approx 54$ meV and $\Delta E_{max,shift} \approx 15$ meV, respectively. A weighted average for CZTSSe with a sulfur content ($[S]/([S]+[Se])$) of around 10% leads to a maximum shift of $\Delta E_{max,shift} \approx 19$ meV. Furthermore, the temperature dependence in DAP transitions should show a shift to higher energies of the PL maximum with increasing temperature at constant excitation power, since more closer pairs are populated, which is in contrast to the observed behavior (Fig. 4) [51]. So the PL transition at low temperature is not a "normal" DAP transition.

2. Quasi-donor-acceptor pair transitions

However, alternatively, the observed behavior could be explained partially by a DAP transition in the presence of fluctuating band edges. The energy of a DAP transition in this case can be calculated by Eq. (6). As described in Sec. I, different mechanisms can create fluctuations of the band edges. DAP transitions in the presence of fluctuating band edges are called quasi-donor-acceptor pair transitions (QDAP transitions). Originally, the QDAP model was introduced for DAP transitions in the presence of EPFs [52] but it can in principle also be used in case of band gap fluctuations. In the QDAP model, the luminescence photon energy is calculated via [52]

$$E = E_g - E_D - E_A - 2\gamma, \tag{6}$$

where E_g is the band gap energy, E_D and E_A are the donor and acceptor binding energies, respectively, and γ is the average depth of the fluctuation. Here, the Coulomb term $\frac{e^2}{4\pi\epsilon_0\epsilon r}$ is neglected (r is the distance between the donor and acceptor and the other symbols have their usual meanings).

In the case of EPFs, the potential depth depends on the screening radius r_s (potential fluctuations on a length scale larger than r_s are screened) and the total concentration of

ionized donors and acceptors N_t [48,49,53]:

$$\gamma \propto \frac{\sqrt{N_t r_s^3}}{r_s} \propto \frac{N_t^{\frac{2}{3}}}{p^{\frac{1}{3}}}, \tag{7}$$

with $r_s \propto N_t^{1/3}/p^{2/3}$ for a p-type semiconductor with the majority carrier density p [25,48,53].

In this sense, the large shift of the PL maximum to higher energies with increasing excitation power is explained by a screening effect. Due to the laser excitation, carriers are generated and they cause a reduction of r_s by a creation of free charge carriers and/or a reduction of the concentration of ionized donors and acceptors. According to Eq. (7), a reduction in r_s due to screening is then accompanied by a reduction in γ. Together with Eq. (6), a reduction in γ translates into an increase in transition energy and hence in a shift of the PL maximum to higher energies.

In a narrower sense, the QDAP model assumes energetically from the valence and concuction bands separated donor and acceptor levels, whereas especially the donor level can merge with the conduction band [52]. The assumption of separate and discrete donor and acceptor levels might not be valid anymore in case of heavily doped and highly compensated semiconductors if the band tailing is too large and the heavy doping condition is satisfied [48]. In this context, the binding energy of a single impurity (especially of a donor) would then have no physical meaning anymore, since discrete impurity levels (donors) hardly exist [20]. Therefore the use of Eq. (6) in case of heavily doped and highly compensated semiconductors, especially the existence of a separate binding energy for the donor, is questionable [20]. Hence E_D would also not be directly accessible by PL measurements.

3. *Luminescence in heavily doped and compensated semiconductors*

The heavy doping condition is satisfied if $N_{a,d}a_{a,d}^3 \gg 1$ with $N_{a,d}$ being the concentration of acceptor and donor impurities and $a_{a,d}$ being the Bohr radius of the impurity state, respectively [53]. To give an example in $Cu_2ZnSnSe_4$ with $m_n^*(\mathrm{Se}) \approx 0.33\, m_0$ and $\epsilon_r(\mathrm{Se}) \approx 8.6$ [54], the Bohr radius will calculate to $a_d \approx 1.4 \times 10^{-7}$ cm. Therefore, for acceptors, the equality $N_d a_d^3 = 1$ is fulfilled for $N_d = 3.8 \times 10^{20}$ cm^{-3}. So heavy doping conditions can realistically be achieved in $Cu_2ZnSnSe_4$ and since the effective mass of the electrons is lower than of the hole, it is already easier fulfilled for donors.

The situation of heavily doped and compensated semiconductors is reviewed by Levanyuk and Osipov [48]. High compensation in a heavily doped semiconductor is generally accompanied by a high density of charged defects. These defects create additional potentials, whereby the band edge is disturbed and EPFs are caused. Luminescence in p-type semiconductors in these cases can be dominated by conduction band tail to valence band tail transitions (TT transitions), by conduction band tail to acceptor impurity transitions (TI transitions), or by various other transitions involving impurities, tail states, and band states [48]. The ratio of occurrence depends on the temperature, the excitation intensity, and whether separate acceptor levels are present or not.

Therefore and additionally since the exact distribution of the DOS within the investigated solar cell absorbers is not known, the assignment of the observed PL transitions to a specific transition is very difficult. For example, TI transitions can be seen as DAP transitions in the case of a heavily doped and compensated semiconductor [48] and are therefore similar to QDAP transitions, which were introduced by Yu as the DAP transition in a compensated semiconductor [52]. So even a distinction between the different transitions is difficult.

However, the physical mechanism responsible for the observed shifting behavior of the PL maximum (a screening effect or a state filling effect) should essentially be nearly independent of the nature of the transition.

C. State filling versus screening in luminescence

So in the following we will have a look how a screening effect can be distinguished from state filling with the techniques presented in this manuscript. The actual shape of the luminescence for the different kinds of transitions mentioned above is not easy to describe, but some basic dependencies can be assessed. (i) A shift of the luminescence maximum towards higher energies with increasing excitation power is expected, e.g., in QDAP, TI, and TT transitions at low temperatures [20,25,48,55]. (ii) The low-energy edge of the luminescence is affected by the tailing parameter [48]. To give an example, in, e.g., TT transitions, the luminescence intensity $\Phi(\omega)$ of the low-energy edge for a random distribution of impurities for low excitation intensity is described by [48,55]

$$\Phi(\omega) \propto \exp\left[-\frac{\left(E_g^0 - \hbar\omega\right)^2}{2\gamma^2}\right], \tag{8}$$

with E_g^0 being the band gap of the undoped material and γ the depth of the potential as described by Eq. (7). The formula can also be used to describe other transitions (band-impurity or band-tail transitions) if the carriers are in quasiequilibrium [18].

Following Eq. (8), a change in the potential depth γ [as expected for a screening effect, Eq. (7)] should lead to a change in the luminescence, especially, a decrease of γ should result in a steeper slope of the low-energy tail of the luminescence.

In case of band edge fluctuations, the shift of the PL maximum to lower energies with increasing temperature can be explained with a higher occupation of deeper valleys or a depopulation of shallower valleys accompanied by an increased non-radiative recombination due to higher mobilities [20,48,56,57]. Due to the increase in temperature, the carriers get more mobile, can leave the local shallow minima and populate deeper minima or recombine more effectively. So the shift of the PL maxima with increasing temperature alone is not sufficient to distinguish band gap fluctuations from EPFs.

However, in case of screening, this shift to lower photon energies should be highly dependent on the excitation power as seen for $Cu(In,Ga)Se_2$ [56,57]. A higher excitation power should result in a reduced fluctuation amplitude γ and thus in a reduced shift to lower energies of the PL maximum as a function of increasing temperature. Compared to that the temperature dependence of the shift of the PL maximum towards lower energies on excitation power should be lower if the potential depth γ is independent of excitation power, as it is the case if the states are filled and no EPFs are screened [56].

Therefore the experimental results of Figs. 1 and 4 are not consistent with a simple screening model of EPFs. Neither the expected change in the low-energy slope of the luminescence due to a reduction of the tailing parameter γ caused by screening nor a dependence of the temperature shifting behavior as a function of the excitation power are observed.[2] Although EPFs may be present to some degree, the experimental data favor another dominant effect for the explanation of the observed luminescence behavior.

D. State filling in CZTSSe

In contrast to a screening effect there is strong evidence that the results presented in this manuscript can be explained more consistently by a state filling effect. The luminescence at low temperatures is dominated by transitions involving a low density of states (Fig. 3). For efficient filling, it is important that the density of the states (DOS) involved in the radiative transition is not too high, so that carriers can fill the states and a filling effect is visible in the emission spectrum. Since we observe some transitions related to traplike states induced by material imperfections with low absorption for the low radiative recombination energies, a rather small joint density of states can be expected, and filling should be very efficient. An increase in excitation power raises the density of nonequilibrium carriers, which can fill the states with a low density [58].

1. Illustrating state filling

To illustrate a filling effect in a very simplistic way, the picture of a funnel can be used. Into a funnel some material, e.g., water, can be dumped from the top and some amount of it will flow out from the bottom. If this picture is translated to a semiconductor, the water would correspond to charge carriers produced by light excitation and the drain of the funnel would correspond to recombination of the carriers. The funnel itself represents the density of states, or more precisely the joint density of states. Due to the additional nonthermal carriers (induced by light excitation in PL measurements), a new dynamic equilibrium will form in which the generation and recombination of carriers equals $R_{eq} = G_{eq}$. Here, R_{eq} is the recombination rate and G_{eq} the generation rate. The same amount of carriers that are dumped into the funnel will flow out at the bottom.

If the laser power, and hence the number of created carriers, is increased, the generation rate exceeds the recombination rate and a state filling occurs. Due to a restricted decay time, the amount of generation is higher than the amount of recombination and hence the density of states is filled. For sure at some point in time a new equilibrium will form for one excitation power since recombination depends also on the number of excited carriers. This state filling is accompanied by a shift of the PL maximum to higher energies. In the funnel picture, this is like dumping more water into the funnel than water that flows out. As a result, the water level inside the funnel will rise—filling occurs. However, at some point, the water level stabilizes since the amount of water that flows out also depends on the height of the water level inside the funnel. Then the amount of water that flows out is again as high as the amount of water that is dumped in.

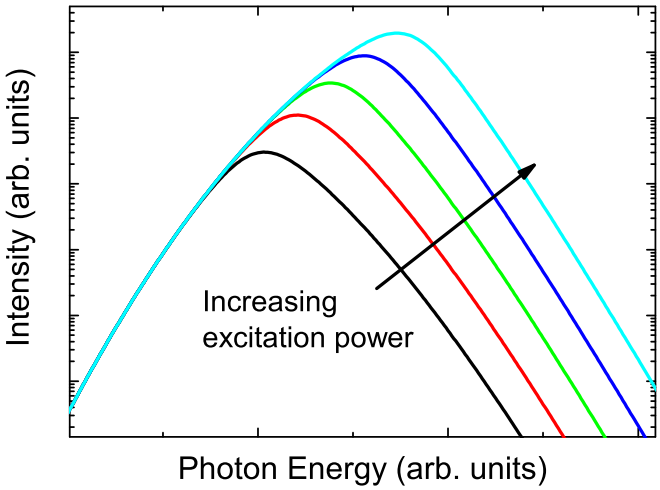

FIG. 5. Modeled PL spectra to illustrate the effect of a state filling on the luminescence. The spectra are calculated using Eq. (9) and the increase in excitation power is simulated with an energetic increase of the distribution function. A shift of the PL maximum to higher energies is observed, whereas the low- and high-energy tail do not change their slope.

Additionally to the shift of the PL maximum, no change of the PL low-energy slope is expected for state filling. This is due to the fact that the JDOS determines the low-energy slope of the PL and since the JDOS is fixed and not altered by the number of excited charge carriers also the low-energy slope of the PL does not change as a function of excitation power. In the funnel picture, the JDOS is represented by the funnel itself and its shape is not altered by the water level inside the funnel. So state filling only changes the occupation, but not the JDOS itself.

This is consistent with the experimental spectra of Fig. 1. A large shift of the PL maximum to higher energies with increasing excitation power is visible, whereas the low-energy slope does not change.

2. Modeling state filling

This is also modeled and illustrated in Fig. 5. In this illustration, PL spectra are simplistically modeled using a product of a JDOS for the valence and conduction band tails and a joint distribution function for both the electrons and holes. The product of a density of states and a distribution function results in an occupation number. In the illustration, the occupation number describes the occupation of radiative transitions which have a radiative transition probability of one, meaning that the energetic distribution of the occupation equals the calculated luminescence spectrum.

Although this simplified model cannot be expected to accurately describe details of the actual photoluminescence of CZTSSe at low temperature it clearly illustrates the effect of state filling. Since it is seen that the absorption and hence also the JDOS has some tailing (Fig. 3), we used a JDOS

[2]It has to be mentioned that the decrease of the energetic position of the PL maximum as a function of increasing temperature cannot be explained by a reduction of E_g with increasing temperature, since the decrease of E_g is expected to be much smaller [59].

calculated from the tailing model of Eq. (4). For a constant transition probability between the initial and the final states, the JDOS can be calculated from the absorption coefficient via $\mathrm{JDOS}(\omega) = \alpha(\omega)\,\hbar\omega$. To illustrate a state filling, the PL spectra were calculated based on the above-mentioned assumptions via

$$\Phi(\omega) \propto \frac{1}{\gamma}\int_0^\infty \frac{1}{\exp\left(\frac{\hbar\omega - E_\mathrm{F}}{k_\mathrm{b}T}\right)+1} \times \exp\left[-\frac{1}{2}\left(\frac{E-\bar{E}_\mathrm{g}}{\gamma}\right)^2\right]\sqrt{\hbar\omega - E}\,dE. \quad (9)$$

Here, E_F is the energy edge of the distribution function up to which the JDOS is filled and T the temperature. Within this model, filling is described by a subsequent occupation of states with increasing number of nonequilibrium carriers. Therefore an increase in excitation power is simulated with an increase in E_F. The temperature in the model was chosen as $T = 100$ K and the used tailing parameter as $\gamma = 41$ meV, which is a reasonable value for CZTSSe based on fitting Eq. (4) to the PLE spectra.

In Fig. 5, the simulated PL spectra are plotted for different values of E_F and hence different excitation powers P. A large shift of the PL maximum to higher energies with an increasing value of E_F is observed, whereas the low and the high energy tails do not change their slope. Comparing the measured spectra of Fig. 1 with the simulation of Fig. 5, a qualitatively similar behavior is observed.

V. CONCLUSION

In conclusion, we have shown by the complementary techniques of PL and PLE that the luminescence of CZTSSe at low temperatures lies energetically far below the absorption edge and is hence related to an energetic region of a low joint density of states. Therefore a state filling with an increase in excitation power can be expected. Indeed, we presented evidence based on a detailed analysis of the full PL line shape, that the power-dependent shift of the luminescence maximum is dominated by state filling rather than by a screening effect. To further support this result, the temperature dependence of the PL for different excitation powers was investigated. It was found that the shift of the PL maximum towards lower energies with increasing temperature at constant excitation power is independent of the excitation power used. This is contradictory to a screening effect for which the shift of the PL maximum as a function of temperature is expected to depend on the excitation power used. The observed temperature dependence and an invariant slope of the low-energy side of the PL as a function of excitation power strongly indicate that the low-energy tailing parameter γ is independent of the excitation power, which is not expected in case of a screening effect. Therefore we conclude that the physical mechanism that dominates the temperature and power dependence of the CZTSSe PL is rather a state filling than a screening effect.

ACKNOWLEDGMENTS

We acknowledge financial support through the Karlsruhe School of Optics and Photonics at KIT (KSOP) and the German Ministry of Education and Research (BMBF), FKZ 03SF0530B. C.K. acknowledges financial support from the Carl-Zeiss Foundation. We would like to thank T. Schnabel, T. Abzieher and E. Ahlswede of the Zentrum für Sonnenenergie- und Wasserstoff-Forschung Baden-Württemberg (ZSW), Stuttgart, Germany for sample fabrication.

[1] Zentrum für Sonnenenergie- und Wasserstoff-Forschung Baden-Württemberg (ZSW), ZSW Sets New World Record for Thin-film Solar Cells (Press Release 09/2016).
[2] R. Kamada, T. Yagioka, S. Adachi, A. Handa, K. F. Tai, T. Kato, H. Sugimoto, in *2016 IEEE 43rd Photovoltaic Specialist Conference (PVSC)* (IEEE, Portland, 2016), pp. 1287–1291.
[3] NREL Efficiency Chart, http://www.nrel.de/pv/assets/images/efficiency_chart.jpg (date of access: 12/19/2016).
[4] W. Wang, M. T. Winkler, O. Gunawan, T. Gokmen, T. K. Todorov, Y. Zhu, and D. B. Mitzi, Adv. Energy Mater. **4**, 1301465 (2014).
[5] S. Siebentritt, Thin Solid Films **535**, 1 (2013).
[6] W. Shockley and H. Queisser, J. Appl. Phys. **32**, 510 (1961).
[7] U. Rau and J. H. Werner, Appl. Phys. Lett. **84**, 3735 (2004).
[8] T. Gokmen, O. Gunawan, T. K. Todorov, and D. B. Mitzi, Appl. Phys. Lett. **103**, 103506 (2013).
[9] S. Schorr, Sol. Energ. Mater. Sol. Cells **95**, 1482 (2011).
[10] T. Washio, H. Nozaki, T. Fukano, T. Motohiro, K. Jimbo, and H. Katagiri, J. Appl. Phys. **110**, 074511 (2011).
[11] M. Paris, L. Choubrac, A. Lafond, C. Guillot-Deudon, and S. Jobic, Inorg. Chem. **53**, 8646 (2014).
[12] J. J. S. Scragg, L. Choubrac, A. Lafond, T. Ericson, and C. Platzer-Björkman, Appl. Phys. Lett. **104**, 041911 (2014).
[13] G. Rey, A. Redinger, J. Sendler, T. P. Weiss, M. Thevenin, M. Guennou, B. El Adib, and S. Siebentritt, Appl. Phys. Lett. **105**, 112106 (2014).
[14] C. Krämmer, C. Huber, C. Zimmermann, M. Lang, T. Schnabel, T. Abzieher, E. Ahlswede, H. Kalt, and M. Hetterich, Appl. Phys. Lett. **105**, 262104 (2014).
[15] J. J. S. Scragg, J. K. Larsen, M. Kumar, C. Persson, J. Sendler, S. Siebentritt, and C. Platzer Björkman, Phys. Status Solidi B **253**, 247 (2015).
[16] S. Chen, A. Walsh, X.-G. Gong, and S.-H. Wei, Adv. Mater. **25**, 1522 (2013).
[17] J. P. Leitão, N. M. Santos, P. A. Fernandes, P. M. P. Salomé, A. F. da Cunha, J. C. González, G. M. Ribeiro, and F. M. Matinaga, Phys. Rev. B **84**, 024120 (2011).
[18] J. Sendler, M. Thevenin, F. Werner, A. Redinger, S. Li, C. Hägglund, C. Platzer-Björkman, and S. Siebentritt, J. Appl. Phys. **120**, 125701 (2016).
[19] T. Gokmen, O. Gunawan, and D. B. Mitzi, Appl. Phys. Lett. **105**, 033903 (2014).

[20] J. P. Teixeira, R. A. Sousa, M. G. Sousa, A. F. da Cunha, P. A. Fernandes, P. M. P. Salomé, and J. P. Leitão, Phys. Rev. B **90**, 235202 (2014).

[21] S. Oueslati, G. Brammertz, M. Buffière, C. Köble, T. Oualid, M. Meuris, and J. Poortmans, Sol. Energy Mater. Sol. Cells **134**, 340 (2015).

[22] X. Lin, A. Ennaoui, S. Levcenko, T. Dittrich, J. Kavalakkatt, S. Kretzschmar, T. Unold, and M. C. Lux-Steiner, Appl. Phys. Lett. **106**, 013903 (2015).

[23] S. Kretzschmar, S. Levcenco, J. Just, A. Redinger, and T. Unold, in *2016 IEEE 43rd Photovoltaic Specialists Conference (PVSC)* (IEEE, Portland, 2016), pp. 0169–0172.

[24] C. J. Hages, N. J. Carter, R. Agrawal, and T. Unold, J. Appl. Phys. **115**, 234504 (2014).

[25] A. Bauknecht, S. Siebentritt, J. Albert, and M. C. Lux-Steiner, J. Appl. Phys. **89**, 4391 (2001).

[26] T. Schnabel, M. Löw, and E. Ahlswede, Sol. Energ. Mater. Sol. Cells **117**, 324 (2013).

[27] C. Krämmer, C. Huber, T. Schnabel, C. Zimmermann, M. Lang, E. Ahlswede, H. Kalt, and M. Hetterich, in *2015 IEEE 42nd Photovoltaic Specialist Conference (PVSC)* (IEEE, New Orleans, 2015).

[28] M. Lang, C. Zimmermann, C. Krämmer, C. Huber, T. Schnabel, T. Abzieher, E. Ahlswede, H. Kalt, and M. Hetterich, in *2015 IEEE 42nd Photovoltaic Specialist Conference (PVSC)* (IEEE, New Orleans, 2015), pp. 1–4.

[29] M. Lang, T. Renz, C. Zimmermann, C. Krämmer, H. Kalt, and M. Hetterich, in *2016 IEEE 43rd Photovoltaic Specialists Conference (PVSC)* (IEEE, Portland, 2016), pp. 0179–0182.

[30] C. Krämmer, C. Huber, A. Redinger, D. Sperber, G. Rey, S. Siebentritt, H. Kalt, and M. Hetterich, Appl. Phys. Lett. **107**, 222104 (2015).

[31] C. Huber, C. Krämmer, D. Sperber, A. Magin, H. Kalt, and M. Hetterich, Phys. Rev. B **92**, 075201 (2015).

[32] J. Krustok, H. Collan, M. Yakushev, and K. Hjelt, Phys. Scripta **T79**, 179 (1999).

[33] K. F. Tai, T. Gershon, O. Gunawan, and C. H. A. Huan, J. Appl. Phys. **117**, 235701 (2015).

[34] P. Yu and M. Cardona, *Fundamentals of Semicondutors*, 1st ed. (Springer-Verlag Berlin, Heidelberg, New York, 1996).

[35] C. Klingshirn, *Semiconductor Optics* (Springer, Berlin and Heidelberg, 2005).

[36] P. W. Yu, C. E. Stutz, M. O. Manasreh, R. Kaspi, and M. A. Capano, J. Appl. Phys. **76**, 504 (1994).

[37] J. P. Teixeira, R. A. Sousa, M. G. Sousa, A. F. da Cunha, P. A. Fernandes, P. M. P. Salomé, J. C. González, and J. P. Leitão, Appl. Phys. Lett. **105**, 163901 (2014).

[38] J. P. Teixeira, R. A. Sousa, M. G. Sousa, A. F. da Cunha, P. A. Fernandes, P. M. P. Salomé, J. C. González, and J. P. Leitão, Appl. Phys. Lett. **107**, 049903(E) (2015).

[39] T. Schmidt, K. Lischka, and W. Zulehner, Phys. Rev. B **45**, 8989 (1992).

[40] W. Grieshaber, E. F. Schubert, I. D. Goepfert, R. F. Karlicek, M. J. Schurman, and C. Tran, J. Appl. Phys. **80**, 4615 (1996).

[41] K. Maeda, J. Phys. Chem. Solids **26**, 595 (1965).

[42] F. Urbach, Phys. Rev. **92**, 1324 (1953).

[43] J. K. Katahara and H. W. Hillhouse, J. Appl. Phys. **116**, 173504 (2014).

[44] J. Mattheis, U. Rau, and J. H. Werner, J. Appl. Phys. **101**, 113519 (2007).

[45] P. Roura, M. López-de Miguel, A. Cornet, and J. R. Morante, J. Appl. Phys. **81**, 6916 (1997).

[46] M. Lang, T. Renz, N. Mathes, M. Neuwirth, T. Schnabel, H. Kalt, and M. Hetterich, Appl. Phys. Lett. **109**, 142103 (2016).

[47] V. P. Dobrego and I. S. Shlimak, Phys. Stat. Solidi **33**, 805 (1969).

[48] A. P. Levanyuk and V. V. Osipov, Sov. Phys. Uspekhi **24**, 187 (1981).

[49] A. L. Éfros, Sov. Phys. Uspekhi **16**, 789 (1974).

[50] E. Zacks and A. Halperin, Phys. Rev. B **6**, 3072 (1972).

[51] D. Abou-Ras, T. Kirchartz, and U. Rau, *in Advanced Characterization Techniques for Thin Film Solar Cells*, edited by D. Abou-Ras, T. Kirchartz, and U. Rau (Wiley-VCH, Weinheim, 2011).

[52] P. W. Yu, J. Appl. Phys. **48**, 5043 (1977).

[53] B. I. Shklovskii and A. L. Efros, *in Electronic Properties of Doped Semiconductors*, edited by M. Cardona, Springer Series in Solid-State Science Vol. 45 (Springer Verlag, Berlin, Heidelberg, New York, Tokyo, 1984).

[54] C. Persson, J. Appl. Phys. **107**, 053710 (2010).

[55] V. V. Osipov, T. I. Soboleva, and M. G. Foigel, Zh. Eksp. Fiz. **75**, 1044 (1978) [Sov. Phys. JETP **48**(3), 527 (1978)].

[56] S. A. Schumacher, J. R. Botha, and V. Alberts, J. Appl. Phys. **99**, 063508 (2006).

[57] I. Dirnstorfer, M. Wagner, D. M. Hofmann, M. D. Lampert, F. Karg, and B. K. Meyer, Phys. Status Solidi A **168**, 163 (1998).

[58] I. Kuskovsky, D. Li, G. F. Neumark, V. N. Bondarev, and P. V. Pikhitsa, Appl. Phys. Lett. **75**, 1243 (1999).

[59] S. Choi, T. Kim, S. Hwang, J. Li, C. Persson, Y. Kim, S.-H. Wei, and I. Repins, Sol. Energ. Mat. Sol. C. **130**, 375 (2014).